

# Voltage-controlled tunable GaAs/AlGaAs multistack quantum well infrared detector

I. Gravé, A. Shakouri, N. Kuze, and A. Yariv

California Institute of Technology, 128-95, Pasadena, California 91125

(Received 6 January 1992; accepted for publication 7 March 1992)

We describe a new type of intersubband GaAs/AlGaAs infrared detector consisting of three stacks of quantum wells; the quantum wells in a given stack are identical, but are different from stack to stack. Each stack is designed to yield an absorption and a photoresponse at a different peak wavelength. The resulting device is an infrared detector which can operate in a number of modes. Among the features of this device are a wide-band detection domain, a tunable response and excellent responsivities and noise figures. The tunable operation includes a sharp peak-switching response which follows the formation, expansion, and readjustment of electric field domains within the multiquantum well region.

Intersubband quantum well detectors have recently been the subject of a considerable research effort;<sup>1-6</sup> properties important for many applications are a wide spectral response,<sup>7</sup> preferably over the atmospheric window 8–12  $\mu\text{m}$  and tunability of the peak wavelength.<sup>8-10</sup>

We report here on the operation of a new type of bound-to-continuum GaAs infrared detector, consisting of three different stacks of quantum wells arranged in series. All the wells in a given stack are identical, but each stack is designed for absorption and detection at a different wavelength, featuring distinct well widths and barrier heights.

The detector can operate in one of a number of modes. At forward and low bias voltages, the response peaks at a single wavelength ( $\sim 1400\text{ cm}^{-1}$ ) and the device functions as a standard bound-to-continuum infrared detector.<sup>2,3</sup> When exceeding a temperature-dependent critical applied voltage, the detector's spectral response switches to a different peak wavelength ( $\sim 1140\text{ cm}^{-1}$ ), while the detection at the previous peak is significantly reduced. At a reverse bias the detection is again centered on the higher energy peak ( $\sim 1400\text{ cm}^{-1}$ ) up to a specific applied voltage; for moderately higher voltages, two peaks yield a significant photoresponse. At still higher values of the reverse voltage a third response peak appears, which results in operation as a wide-band detector. These features are accompanied by good responsivity and detectivity figures.

The structure was grown by molecular beam epitaxy on a semi-insulating GaAs substrate. The superlattice, clad by two  $n$ -doped contact layers, consisted of three stacks of 25 quantum wells each; the first 25 wells were 3.9 nm wide and were separated by  $\text{Al}_{0.38}\text{Ga}_{0.62}\text{As}$  barriers; the second stack consisted of 25 quantum wells 4.4 nm wide with  $\text{Al}_{0.30}\text{Ga}_{0.70}\text{As}$  barriers; the last stack had 25 wells 5.0 nm wide and  $\text{Al}_{0.24}\text{Ga}_{0.76}\text{As}$  barriers. All the barriers were 44 nm long; the wells and the contacts were uniformly doped with Si to  $n=4\times 10^{18}\text{ cm}^{-3}$ .

The absorption at zero field and room temperature is shown in Fig. 1. The measurement was taken with a Fourier transform infrared spectrometer in a waveguide geometry;<sup>11</sup> the absorption of light polarized in compliance with the selection rules was normalized by the absorption of

light polarized in the perpendicular direction, to allow for only the intersubband contribution. The absorption peak at  $1364\text{ cm}^{-1}$  is due to the 3.9 nm wells while the stronger absorption centered at  $964\text{ cm}^{-1}$  is the composite contribution of the two other species of quantum well, which, individually, have absorption peaking at 1080 and  $920\text{ cm}^{-1}$ . (This was verified experimentally with a few two-stack control wafers). These results fit well with our design values; our calculations, which included band nonparabolicity<sup>12</sup> and a band offset value of 0.60, anticipated absorption peaks at room temperature at 1335, 1052, and  $880\text{ cm}^{-1}$ , respectively. In each of the three different types of wells, light is absorbed by electrons excited from the first subband to a second subband which is located close to the top of the well. The blue shift in the experimental values versus the calculated ones can be explained by the omission of the exchange interaction<sup>13</sup> from our calculation; for these heavily doped samples, the correction supplied by many-body effects need be added.

Devices were processed out of the grown wafer and prepared as etched mesa, 200  $\mu\text{m}$  in diameter. Figure 2(a)

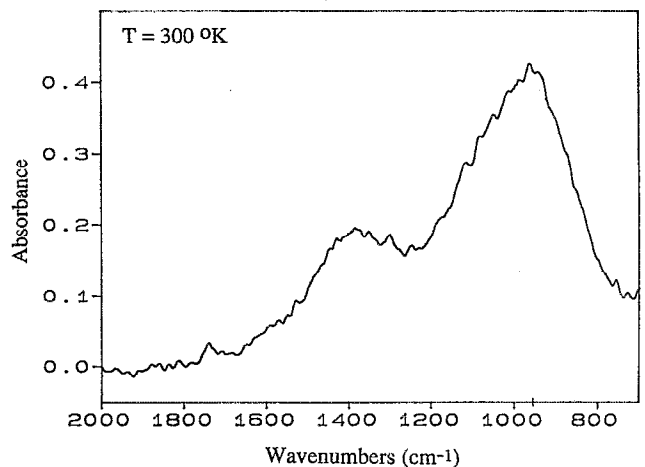


FIG. 1. Absorption spectrum at room temperature. The measurement was performed with a Fourier transform spectrometer using a waveguide geometry; the spectrum is normalized to reflect the contribution of the intersubband absorption alone. An absorption coefficient  $\alpha_{45}=600\text{ cm}^{-1}$  for the peak at  $1364\text{ cm}^{-1}$  was derived.

Report Documentation Page				Form Approved OMB No. 0704-0188	
Public reporting burden for the collection of information is estimated to average 1 hour per response, including the time for reviewing instructions, searching existing data sources, gathering and maintaining the data needed, and completing and reviewing the collection of information. Send comments regarding this burden estimate or any other aspect of this collection of information, including suggestions for reducing this burden, to Washington Headquarters Services, Directorate for Information Operations and Reports, 1215 Jefferson Davis Highway, Suite 1204, Arlington VA 22202-4302. Respondents should be aware that notwithstanding any other provision of law, no person shall be subject to a penalty for failing to comply with a collection of information if it does not display a currently valid OMB control number.					
1. REPORT DATE <b>JAN 1992</b>		2. REPORT TYPE		3. DATES COVERED <b>00-01-1992 to 00-01-1992</b>	
4. TITLE AND SUBTITLE <b>Voltage-controlled tunable GaAs/AlGaAs multistack quantum well infrared detector</b>				5a. CONTRACT NUMBER	
				5b. GRANT NUMBER	
				5c. PROGRAM ELEMENT NUMBER	
6. AUTHOR(S)				5d. PROJECT NUMBER	
				5e. TASK NUMBER	
				5f. WORK UNIT NUMBER	
7. PERFORMING ORGANIZATION NAME(S) AND ADDRESS(ES) <b>California Institute of Technology, Department of Applied Physics, Pasadena, CA, 91125</b>				8. PERFORMING ORGANIZATION REPORT NUMBER	
9. SPONSORING/MONITORING AGENCY NAME(S) AND ADDRESS(ES)				10. SPONSOR/MONITOR'S ACRONYM(S)	
				11. SPONSOR/MONITOR'S REPORT NUMBER(S)	
12. DISTRIBUTION/AVAILABILITY STATEMENT <b>Approved for public release; distribution unlimited</b>					
13. SUPPLEMENTARY NOTES					
14. ABSTRACT					
15. SUBJECT TERMS					
16. SECURITY CLASSIFICATION OF:			17. LIMITATION OF ABSTRACT	18. NUMBER OF PAGES <b>3</b>	19a. NAME OF RESPONSIBLE PERSON
a. REPORT <b>unclassified</b>	b. ABSTRACT <b>unclassified</b>	c. THIS PAGE <b>unclassified</b>			

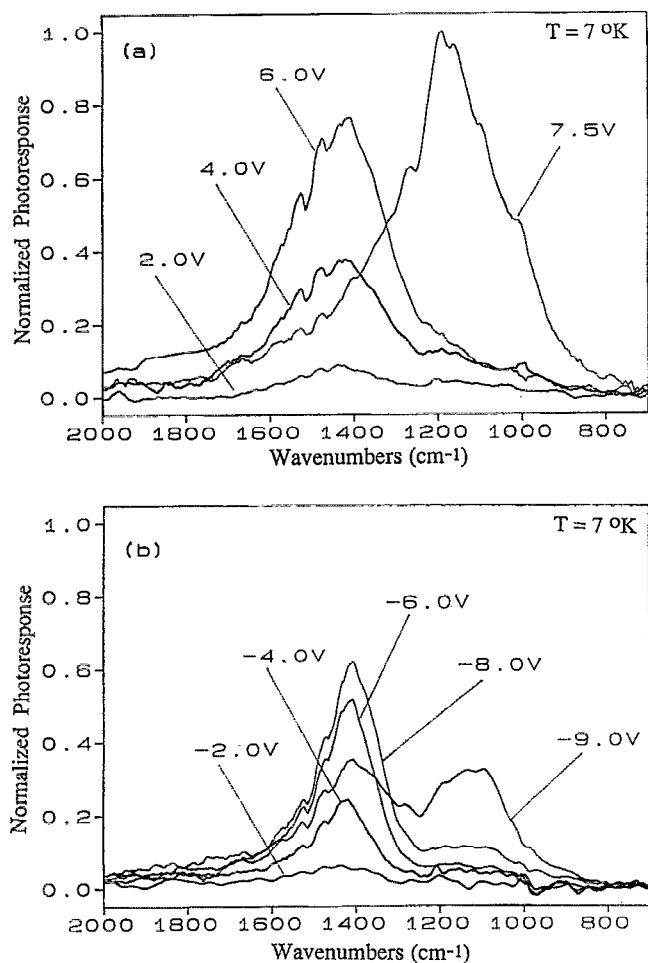


FIG. 2. (a) Spectral photoresponse for few values of applied positive voltage. Note the switching in peaks at an applied voltage around 6.5 V. The responsivity, at the peak of  $1140\text{ cm}^{-1}$  and the applied voltage of 7.5 V, is  $0.75\text{ A/W}$ . (b) Spectral photoresponse for few values of applied negative voltage. Note the broadening in the spectral response below  $-8.0\text{ V}$ . For still lower voltages (around  $-13\text{ V}$ ), the third peak begins to contribute (not shown in the figure). The units are the same for both (a) and (b).

displays the smoothed responsivity of a device at a temperature of 7 K, for different values of the applied voltage; the polarity is defined here as positive when the higher potential is applied to the cap layer on top of the mesa. It is seen that, for low applied field, the first stack of 3.9 nm wells, closer to the substrate, provides most of the photocurrent at the appropriate excitation energies around the peak of  $1411\text{ cm}^{-1}$ . When the bias is increased above a threshold of 6.5 V, a sharp transition takes place and the responsivity peak switches to  $1140\text{ cm}^{-1}$ ; it is apparent that the second stack of quantum wells is now responsible for most of the photocurrent, while the contribution from the first stack has sensibly decreased. If we apply a negative bias to the detector [Fig. 2(b)], again at low voltages, the photocurrent is due mostly to electrons excited in the first stack of wells; the responsivity increases with the applied voltage, but its magnitude is always less than that corresponding to the same forward bias. In addition, one observes that the photocurrent peak around  $1400\text{ cm}^{-1}$  is much broader in the forward bias mode. When the bias is increased to more negative values, the responsivity extends to lower energies,

showing increasing contributions from the second stack: the first stack continues to contribute to the photocurrent, in contrast to the quenching in response experienced in the opposite polarity of the applied electric field. For still more negative voltages, it is apparent from our results that the spectral domain of significant response expands to still lower energies, to include contributions from the third stack of wells, around  $900\text{ cm}^{-1}$ .

We interpret this switching behavior as due to the formation, expansion, and readjustment of stable high and low field domains along the superlattice, as the applied voltage is changed. When the device is biased with a positive polarity, a high field domain is created in the region close to the contact electrode within the first stack of quantum wells; as the applied voltage is increased, the domain spreads to include more and more of the 25 wells in the stack, while a complementary low field domain in the same stack shrinks progressively. At the same time the remaining two stacks of quantum wells experience only low field domains all along their extent. Thus, photons of all appropriate energies are absorbed by the correspondingly matched, highly doped quantum wells; however only electrons excited within the high field regions are swept efficiently towards the contacts and contribute to the photocurrent. The carriers excited in the region of low field have a high probability of being recaptured by their own well, contributing only negligibly to the current. Once the applied voltage reaches a value large enough to extend a high field domain to as many of the 25 wells in the first stack as allowed, the corresponding responsivity reaches its maximum value. When the applied voltage is increased further, a high field domain spreads to the region of the following 25 wells of the second stack, while at the same time quenching of the high field domain in the first stack occurs. Response from a third peak, corresponding to the third stack, was not achieved even at the highest values of the applied forward voltage, indicating that the spatial region of the last stack is always in a low field domain. When the bias is applied with the opposite negative polarity, the situation is not symmetric. The results show that high field domains start expanding, as before, in the region of the first stack of quantum wells; moreover beyond a certain magnitude of the applied voltage, different high field domains coexist in two different stacks, and ultimately, at still higher applied bias, a third high field domain forms—also in the last stack of wells. This behavior, shown in Fig. 2 for the temperature of 7 K, persists at higher temperatures. In the reverse bias direction, one observes the same features also at 77 K. In the forward direction the switching of the photoresponse from the higher energy peak to the lower one is observed up to a temperature of 60 K; the critical voltage at which the switching occurs increases with temperature; at higher temperatures the dark current at the required voltages is too high for practical detection purposes.

The dark current, measured with a cold shielded window is shown at different temperatures in Fig. 3. A fine structure in the plateaux of the  $I$ - $V$  curves (not resolved in Fig. 3), corresponding to regions of negative resistance,

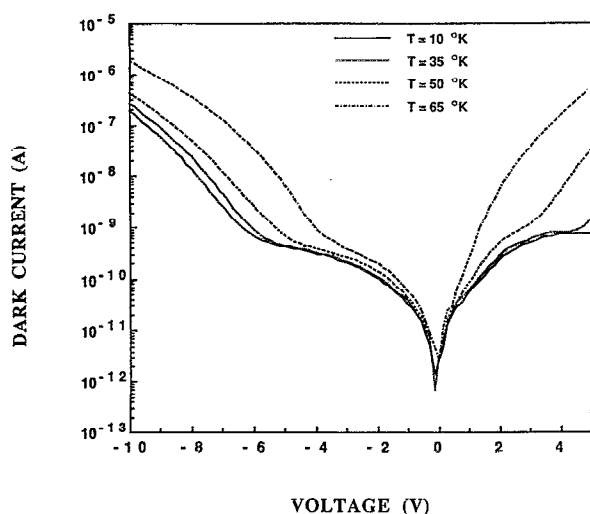


FIG. 3. Dark currents at different temperatures.

was observed and is due to sequential resonant tunneling; negative differential resistance occurs whenever some excited subband in one well is aligned, by the spreading electric field, with the ground state first subband in the adjacent well. One should also note the low values of the dark current, which, combined with a responsivity ranging up to 0.75 A/W, ultimately yield high  $D^*$  for this detector ( $D^* = 4 \times 10^{11} \text{ cm}^2 \text{ Hz}^{1/2} \text{ W}^{-1}$  at 40 K and  $1140 \text{ cm}^{-1}$ ).

The data of the photocurrent spectral measurements were taken with a Fourier transform spectrometer, complemented by a setup including a calibrated black-body source and a set of cooled filters for different wavelength. The noise equivalent voltage was measured with a spectrum analyzer in the cold, shielded window configuration.

The first observation of electric field domain in superlattices was reported by Esaki and Chang.<sup>14</sup> In recent years there have been additional evidences of high field domain formation in various superlattices.<sup>15-17</sup> Most experimental evidences come from the observation of a fine periodic structure in the current-voltage characteristics similar to our observations. Recently, photoluminescence spectroscopy has been used as a tool to complementarily investigate the pattern of high field formation in GaAs/AlGaAs superlattices.<sup>17</sup>

An analysis of the domain switching behavior of our device at the various forward and reverse bias voltages is needed for an understanding of the different detector regimes, and especially of the observed quenching of high field domain in the first stack of quantum wells as the voltage is raised above the switching value of 6.5 V. Such an analysis is beyond the scope of this letter and will be presented separately. One should note, however, that the large switching voltage of 6.5 V across 25 periods, as observed in the photocurrent measurements, corresponds to 260 meV/period. This is much larger than the excited state-ground state separation ( $E_2-E_1$ ) of  $1364 \text{ cm}^{-1}$  (or 169 meV) as inferred from absorption measurements. This seems to indicate that the voltage drop across a low field domain period is nonzero (in agreement with a nonzero linewidth of the subband); more importantly, it also shows

that the energy separation involved in the sequential tunneling transport process is larger than that involved in the absorption process; in other words the transport relies heavily on energy states which are higher in the continuum, above the top of the well.

In conclusion, we describe a new type of intersubband detector. Among the features of the detector are a wide spectral response and a tunable voltage-controlled multi-spectral response. The performances of the detector in terms of responsivity and detectivity are comparable to the best values previously reported for bound-to-continuum detectors. In addition, we have attributed the special switching properties of this device to the formation and readjustment of high field domains in the sample. Finally we have shown that intersubband current spectroscopy is a valid addition to the experimental tools used in studying electric field domains in doped or otherwise carrier-rich structures.

The authors would like to acknowledge the important contribution of Timothy N. Krabach and Susan M. Dejesky at the Jet Propulsion Laboratory, in the detector characterization.

This work was supported by the Defense Advanced Research Projects Agency (DARPA) and the Office of Naval Research.

- <sup>1</sup>J. S. Smith, L. C. Chiu, S. Margalit, A. Yariv, and A. Y. Cho, *J. Vac. Sci. Technol. B* **1**, 376 (1983).
- <sup>2</sup>B. F. Levine, C. G. Bethea, G. Hasnain, J. Walker, and R. J. Malik, *Appl. Phys. Lett.* **53**, 296 (1988).
- <sup>3</sup>B. F. Levine, C. G. Bethea, G. Hasnain, V. O. Shen, E. Pelve, R. R. Abbott, and S. J. Hsieh, *Appl. Phys. Lett.* **56**, 851 (1990).
- <sup>4</sup>H. C. Liu, M. Buchanan, Z. R. Wasilewski, and H. Chu, *Appl. Phys. Lett.* **58**, 1059 (1991).
- <sup>5</sup>H. Schneider, F. Fuchs, B. Dischler, J. D. Ralston, and P. Koidl, *Appl. Phys. Lett.* **58**, 2234 (1991).
- <sup>6</sup>M. A. Kinch and A. Yariv, *Appl. Phys. Lett.* **55**, 2093 (1989).
- <sup>7</sup>B. F. Levine, G. Hasnain, C. G. Bethea, and N. Chand, *Appl. Phys. Lett.* **54**, 2704 (1989).
- <sup>8</sup>K. K. Choi, B. F. Levine, C. G. Bethea, J. Walker, and R. J. Malik, *Phys. Rev. B* **39**, 8029 (1989).
- <sup>9</sup>S. R. Parihar, S. A. Lyon, M. Santos, and M. Shayegan, *Appl. Phys. Lett.* **55**, 2417 (1989).
- <sup>10</sup>B. F. Levine, C. G. Bethea, V. O. Shen, and R. J. Malik, *Appl. Phys. Lett.* **57**, 383 (1990).
- <sup>11</sup>B. F. Levine, R. J. Malik, J. Walker, K. K. Choi, C. G. Bethea, D. A. Kleinman, and J. M. Vandenberg, *Appl. Phys. Lett.* **50**, 273 (1987).
- <sup>12</sup>Z. Y. Xu, V. G. Kreismanis, and C. L. Tang, *Appl. Phys. Lett.* **43**, 415 (1983).
- <sup>13</sup>J. W. Choe, B. O. K. M. S. V. Bandara, and D. D. Coon, *Appl. Phys. Lett.* **56**, 1679 (1990).
- <sup>14</sup>L. Esaki and L. L. Chang, *Phys. Rev. Lett.* **33**, 495 (1974).
- <sup>15</sup>Y. Kawamura, K. Wakita, H. Asahi, and K. Kurumada, *Jpn. J. Appl. Phys.* **25**, L928 (1986); Y. Kawamura, K. Wakita, and K. Oe, *ibid.* **26**, L1603 (1987).
- <sup>16</sup>K. K. Choi, B. F. Levine, R. J. Malik, J. Walker, and C. G. Bethea, *Phys. Rev. B* **35**, 4172 (1987); K. K. Choi, B. F. Levine, C. G. Bethea, J. Walker, and R. J. Malik, *Appl. Phys. Lett.* **50**, 1814 (1987).
- <sup>17</sup>H. T. Grahn, H. Schneider, and K. von Klitzing, *Phys. Rev. B* **41**, 2890 (1990); and references listed therein.